On Equalization Performance in Underwater Acoustic Communication

Vinicius M. Pinho, Rafael S. Chaves, Marcello L. R. Campos

***Abstract*— This paper presents the results of a practical experiment of underwater acoustic transmission, which was performed in Arraial do Cabo, RJ. The primary focus of this experiment is analyzing the performance of different types of equalizers, namely: zero-forcing (ZF), minimum mean square error (MMSE) and decision feedback equalizer (DFE). The mean square error (MSE) and bit-error rate (BER) are the figures of merit used to compare their performances. Results show that in terms of MSE, the DFE has better performance than the other equalizers, achieving an MSE of -25.6 dB for signal-to-noise ratio (SNR) equal to 10 dB. Furthermore, the DFE outperformed the ZF and MMSE equalizers, improving BER by 5.3 dB with respect to the ZF equalizer, and 3.4 dB with respect to the MMSE equalizer.**

***Keywords*— Underwater acoustic, experimental transmission, bit-error rate, equalization, ZF, MMSE, DFE.**

I. Introduction

Underwater communication is deeply rooted in numerous applications. Example of applications can be found in a diversity of areas, from scientific biological research to commercial oil exploration, including governmental coast defense, marine animal protection, and climate change studies. These activities have driven submarine communication studies further, looking for the best solution for every type of application. Underwater communication can use three different types of transmission, namely: acoustic, radio frequency, and optical, each one has its own applicabilities. However, in the underwater environment, acoustic transmission is capable of reaching higher distances than electromagnetic radio frequency or optical transmissions [1], [2]. This feature makes acoustic communication the dominant technology for wireless underwater transmission [1], [3].

Besides being a predominant technology, underwater acoustic (UWA) systems have a plethora of problems that hinder its performance and need to be adequately dealt with. These impairments are related to UWA noise [4] and the intense time variations of UWA channels [5]. Moreover, the relative motion between transmitter and receiver, always present in this environment, combined with the low propagation speed of the acoustic waves, aggravates the Doppler effect [2], [6], [7]. Furthermore, the available bandwidth is limited due to the transmission loss, which increases with both frequency and range and restrains high rate transmissions [8].

Vinicius M. Pinho, Rafael S. Chaves, Marcello L. R. Campos are with Federal University of Rio de Janeiro (UFRJ) / Polytechnic School (Poli) / Department of Electronic and Computer Engineering (DEL) / Signal Multimedia and Telecommunications (SMT), Rio de Janeiro - RJ, Brazil, E-mails: {vinicius.pinho, rafael.chaves, campos}@smt.ufrj.br. The authors are grateful for the financial support provided by CNPq, and FINEP (Comunicações Submarinas FINEP-01.13.0421.00).

In general, the UWA channel is modeled as a time-variant linear system due to the Doppler effect [9]. However, in a situation where the Doppler effect can be neglected, the UWA channel becomes a time-invariant system, and the most predominant impairment becomes intersymbol interference (ISI). ISI is mostly induced by the time spread in the received acoustic signal due to the multiple interactions of the signal with sea surface and bottom. As in radio frequency wireless communication in the air, ISI is also harmful in UWA communication and must be appropriately compensated by the transceiver [8]. One of the tools used for mitigating ISI is called channel equalization, which uses some knowledge of the channel state or its impulse response.

From a probability of error viewpoint, the maximum likelihood sequence equalizer is optimum [10]. However, the computational complexity of the maximum likelihood sequence equalizer increases exponentially with channel length, being unpractical in embedded systems [11]. In order to reduce the computational load, suboptimal solutions consisting of linear filters are often employed, such as the zero-forcing (ZF) [10], [11] and minimum mean square error (MMSE) equalizers [10], [11]. Another solution is the decision feedback equalizer (DFE), which exploits the use of previously estimated symbols to reduce ISI [12]. Even though it is not linear, the DFE does not have high complexity and achieves a better performance than ZF and MMSE equalizers in terms of bit-error rate (BER) [13].

This paper presents a study on the performance of the ZF equalizer, the MMSE equalizer, and the DFE applied to practical experimental data of UWA communication. This practical experiment was carried out in cooperation with the Institute of Sea Studies Admiral Paulo Moreira (IEAPM) at Enseada dos Anjos in Arraial do Cabo, RJ. Practical experiments present new challenges that may not be properly modeled in simulations. Such as those imposed by the real UWA channel.

This paper is organized as follows: Section II describes a general model of a UWA transceiver in baseband. Section III presents a description of the three equalizers employed in this work: ZF equalizer, MMSE equalizer, and DFE. Section IV describes the design of the transceiver used in the experiment, whereas Section V shows the results that arose from processing the received data using the equalizers from Section III. Finally, Section VI draws some conclusions about the performances of the equalizers used in the practical experiment.

Notation: Vectors and matrices are represented in bold face with lowercase and uppercase letters, respectively. The notations $[\cdot]^{\mathrm{T}}$, $[\cdot]^{\mathrm{H}}$, $[\cdot]^{-1}$ stand for transpose, transpose conjugate

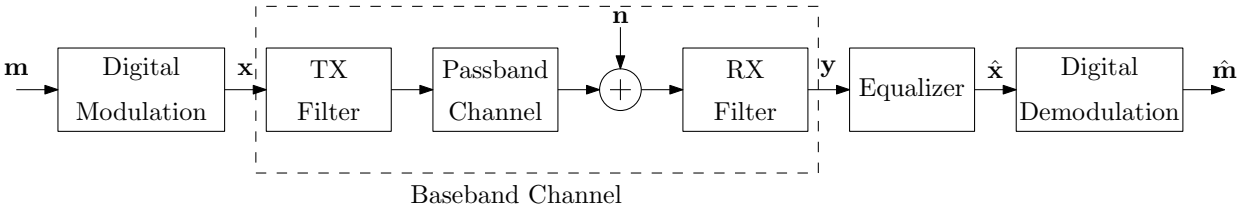

Fig. 1. Baseband model for the UWA transceiver.

and inverse operations on $[\cdot]$, respectively. The symbols $\mathbb{N}$, $\mathbb{R}$, $\mathbb{C}$ denote the set of natural, real, and complex numbers, respectively. The set of $\mathbb{C}^{M\times N}$ denotes all $M \times N$ matrices comprised of complex-valued entries. The symbols $\mathbf{0}_{M\times N}$, $\mathbf{I}_M$ denote an $M \times N$ matrix with zeros and the $M \times M$ identity matrix, respectively.

II. System Model

Let a simplified UWA transceiver be as illustrated in Fig. 1. Consider the data block $\mathbf{x} \in \mathcal{C}^{N\times 1} \subset \mathbb{C}^{N\times 1}$ containing $N \in \mathbb{N}$ symbols of a generic constellation $\mathcal{C}$. This data block is prepared to be transmitted through a UWA multipath channel with baseband finite transfer function denoted as

$$H(z) = \sum_{l\in\mathcal{L}} h_l z^{-l}, \tag{1}$$

where $\mathcal{L} = \{1,\ 2,\ \cdots,\ L\}$ is the set containing all the multipath indexes, and h_l is the lth coefficient in time domain. For a matrix analysis, the baseband channel can be written as a Toeplitz matrix given by

$$\mathbf{H} = \begin{bmatrix} h_1 & 0 & \cdots & 0 & 0 \\ h_2 & h_1 & \cdots & 0 & 0 \\ \vdots & \vdots & \cdots & \vdots & \vdots \\ h_L & h_{L-1} & \cdots & 0 & 0 \\ 0 & h_L & \cdots & 0 & 0 \\ \vdots & \vdots & \vdots & \vdots & \vdots \\ 0 & 0 & \cdots & h_{L-1} & h_{L-2} \\ 0 & 0 & \cdots & h_L & h_{L-1} \\ 0 & 0 & 0 & \cdots & h_L \end{bmatrix} \in \mathbb{C}^{M\times N}, \tag{2}$$

where $M = N + L - 1$. The received signal is denoted as

$$\mathbf{y} = \mathbf{H}\mathbf{x} + \mathbf{n}, \tag{3}$$

where $\mathbf{y} \in \mathbb{C}^{M\times 1}$ is the received signal, and $\mathbf{n} \in \mathbb{C}^{M\times 1}$ is the additive white Gaussian noise (AWGN). The UWA multipath channel induces ISI, which degrades the quality of the received signal. Thus, in order to recover the original message, the receiver must equalize the received signal to mitigate the effects of the channel. The estimated signal $\hat{\mathbf{x}}$ is given by

$$\hat{\mathbf{x}} = \mathbf{W}\mathbf{H}\mathbf{x} + \mathbf{W}\mathbf{n}. \tag{4}$$

where $\mathbf{W} \in \mathbb{C}^{N\times M}$ is the equalization matrix.

The equalizer is a crucial part of the receiver and a standard tool to tackle the ISI generated by the channel. The equalizer can dramatically improve the performance of the transceiver and will be appropriately defined in Section III.

III. Equalization

Equalization is a method that generates estimates of the transmitted signal by compensating channel effects. There are different approaches for this compensation, such as directly inverting the channel, or minimizing the mean square error (MSE) between the estimated and transmitted symbol [10]. Moreover, equalization can be linear or nonlinear, having a trade-off between complexity and performance. In general, nonlinear equalizers achieve lower BER than linear equalizers, but at the expense of higher complexity when compared to linear equalizers.

A. Zero-forcing Equalizer

The ZF equalizer is a solution for mitigating the ISI that tries to restore the Nyquist Criterion for an free ISI transmission by inverting the channel matrix [11]. The ZF equalizer overlooks the additive noise, and solves the problem $\mathbf{y} = \mathbf{H}\hat{\mathbf{x}}$. Therefore, the estimated data block $\hat{\mathbf{x}}$ is given

$$\hat{\mathbf{x}} = \underbrace{(\mathbf{H}^{\mathrm{H}}\mathbf{H})^{-1}\mathbf{H}^{\mathrm{H}}}_{\mathbf{W}_{\mathrm{ZF}}}\mathbf{y}. \tag{5}$$

One of the drawbacks regarding this equalizer is ignoring the effect of additive noise, which may lead to overall performance degradation due to noise enhancement. For example, if the channel has a spectral null containing only background noise in its frequency response, the ZF equalizer attempts to compensate for this by introducing a large gain at that frequency.

B. Minimum Mean Square Error Equalizer

A solution to overcome the noise enhancement caused by the ZF equalizer is the use of MMSE equalizer [11], which takes into account the additive noise for data block estimation. The MSE between the transmitted and estimated data blocks is used to derive the equalizer coefficients. Thus, the MMSE equalizer matrix [14] is

$$\mathbf{W}_{\mathrm{MMSE}} = \underset{\mathbf{W}\in\mathbb{C}^{N\times M}}{\operatorname{argmin}}\ \mathsf{E}\left[\|\mathbf{x} - \mathbf{W}\left(\mathbf{H}\mathbf{x} + \mathbf{n}\right)\|_2^2\right], \tag{6}$$

and, the estimated data block $\hat{\mathbf{x}}$ becomes

$$\hat{\mathbf{x}} = \underbrace{\left(\mathbf{H}^{\mathrm{H}}\mathbf{H} + \frac{1}{\mathrm{SNR}}\mathbf{I}_N\right)^{-1}\mathbf{H}^{\mathrm{H}}}_{\mathbf{W}_{\mathrm{MMSE}}}\mathbf{y}, \tag{7}$$

where $\mathsf{E}[\cdot]$ is the expected value operator.

There are similarities between the expressions for computing the MMSE and the ZF equalizers. In high SNR regime, $\mathbf{W}_{\mathrm{MMSE}}$ is close to $\mathbf{W}_{\mathrm{ZF}}$. Moreover, for low SNR regime, the

regularization by SNR copes with noise enhancement holding up the equalizer from introducing large gains when the channel has a signal spectral null in its frequency response.

C. Decision Feedback Equalizer

Decision feedback equalizer is a nonlinear equalizer that uses past estimated symbols to make a better decision on the current symbol [13], [15]. The equalization performed by DFE is carried out symbol-by-symbol. The main idea of DFE is to feed back already equalized symbols through a filter to improve the equalization of the current symbol. Any remaining ISI caused by a previous symbol is reconstructed and then subtracted. The DFE is inherently a nonlinear device, but by assuming that all the previous decisions were made correctly, the analysis can be linear [13]. The finite-length DFE consists of a forward filter $\mathbf{w} \in \mathbb{C}^{F\times 1}$ given by $\mathbf{w} = [\, w_{-(F-1)} \ \cdots \ w_{-1} \ w_0 \,]^{\mathrm{H}}$, and a feedback filter $\mathbf{b} \in \mathbb{C}^{B+1\times 1}$, written as $\mathbf{b} = [\, 1 \ b_1 \ \cdots \ b_B \,]^{\mathrm{H}}$.

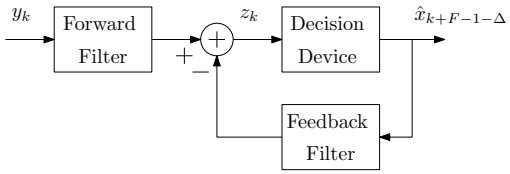

Fig. 2. Structure for decision feedback equalizer.

To obtain the optimum forward and feedback filters, we need to minimize the MSE at the input of the decision device. The error between the correct symbol $x_{k+F-1-\Delta}$ and input z_k at the decision device is given by

$$\begin{aligned} e_k &= x_{k+F-1-\Delta} - z_k \\ &= \underbrace{\begin{bmatrix}\mathbf{0}_{1\times\Delta} & \mathbf{b}^{\mathrm{H}} & \mathbf{0}_{1\times S}\end{bmatrix}}_{\tilde{\mathbf{b}}^{\mathrm{H}}} \mathbf{x}_k - \mathbf{w}^{\mathrm{H}}\mathbf{y}_k, \end{aligned} \tag{8}$$

where

$$\mathbf{x}_k = [\, x_{k+F-1} \ x_{k+F} \ \cdots \ x_{k-(L-1)} \,]^{\mathrm{T}} \tag{9}$$

is the correct symbol vector at instant k,

$$\mathbf{y}_k = [\, y_{k+F-1} \ y_{k+F} \ \cdots \ y_k \,]^{\mathrm{T}} \tag{10}$$

the received symbol vector at instant k.

The constant S in (8) is given by $S = F - 1 - \Delta$, where Δ is the decision delay inherent in a causal DFE, satisfying $0 \le \Delta \le F+L-2$. The optimum Δ is given by $\Delta_{\mathrm{opt}} = F-1$, leading to $S = 0$. The length of the forward and feedback filters are related to the length of the channel. Furthermore, the DFE performance is enhanced with $F = 2L-2$ and $B = L-1$ [16].

In order to find the forward and backward filter coefficients, we need to compute the MSE of (8), written as

$$\begin{aligned} \xi &= \mathsf{E}\left[|e_k|^2\right] \\ &= \tilde{\mathbf{b}}^{\mathrm{H}}\mathbf{R}_{xx}\tilde{\mathbf{b}} - \tilde{\mathbf{b}}^{\mathrm{H}}\mathbf{R}_{xy}\mathbf{w} - \mathbf{w}^{\mathrm{H}}\mathbf{R}_{yx}\tilde{\mathbf{b}} + \mathbf{w}^{\mathrm{H}}\mathbf{R}_{yy}\mathbf{w}, \end{aligned} \tag{11}$$

where $\mathbf{R}_{xx} = \mathsf{E}\left[\mathbf{x}\mathbf{x}^{\mathrm{H}}\right]$, $\mathbf{R}_{nn} = \mathsf{E}\left[\mathbf{n}\mathbf{n}^{\mathrm{H}}\right]$, $\mathbf{R}_{xy} = \mathbf{R}_{xx}\mathbf{H}^{\mathrm{H}}$, and $\mathbf{R}_{yy} = \mathbf{H}\mathbf{R}_{xx}\mathbf{H}^{\mathrm{H}} + \mathbf{R}_{nn}$. By the orthogonality principle [13], the following relation holds

$$\tilde{\mathbf{b}}^{\mathrm{H}}\mathbf{R}_{xy} = \mathbf{w}^{\mathrm{H}}\mathbf{R}_{yy}. \tag{12}$$

Then, by (11) and (12), the MSE can be rewritten as

$$\xi = \mathbf{b}^{\mathrm{H}}\mathbf{R}_{\Delta}\mathbf{b}, \tag{13}$$

where $\mathbf{R}_{\Delta} = \mathbf{Q}\left(\mathbf{R}_{xx}^{-1} + \mathbf{H}^{\mathrm{H}}\mathbf{R}_{nn}^{-1}\mathbf{H}\right)^{-1}\mathbf{Q}^{\mathrm{T}}$ and $\mathbf{Q} = \begin{bmatrix}\mathbf{0}_{(B+1)\times\Delta} & \mathbf{I}_{(B+1)} & \mathbf{0}_{(B+1)\times S}\end{bmatrix}$. Equation (13) is a quadratic form that is minimized by choosing the feedback filter as

$$\mathbf{b} = \frac{\mathbf{R}_{\Delta}^{-1}\mathbf{e}_1}{\mathbf{e}_1^{\mathrm{T}}\mathbf{R}_{\Delta}^{-1}\mathbf{e}_1}, \tag{14}$$

yielding

$$\mathbf{w}^{\mathrm{H}} = \tilde{\mathbf{b}}^{\mathrm{H}}\mathbf{R}_{xy}\mathbf{R}_{yy}^{-1}, \tag{15}$$

where $\mathbf{e}_1$ is the first column of $\mathbf{I}_{B+1}$.

IV. Practical Experiment

A. Experimental Transmission Settings

The testbed used for the practical experiment consists of a transmitter and a receiver. Both transmitter and receiver have digital back-end and analog front-end parts. The analog front-end transmitter receives an audio file from the digital back-end transmitter. First, this file is converted into an acoustic signal that is filtered by an analog bandpass filter (5-10 kHz). After this, the resulting signal is transmitted through the UWA channel. At the receiver, the analog front-end converts the received acoustic signal into an audio file sampled with $f_{\mathrm{s}} = 96$ kHz and supplies this file to the digital back-end receiver.

The experiment took place at Enseada dos Anjos, which is a bay in Arraial do Cabo. The experiment setup consisted of a vessel that remained anchored throughout the experiment, and it held the transmitter 20 m below the sea surface. The receiver was anchored to the ocean bottom near the coast, at a depth of 10 m and 250 m away from the transmitter. The experiment setup is illustrated in Fig 3.

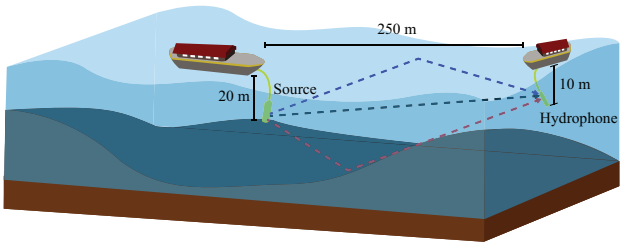

Fig. 3. Illustration of the experiment setup.

B. Digital Transmitter

In the digital back-end transmitter, the original message consists of a ten-by-ten pixel image. This image is converted into a bit stream, which is encoded by a convolutional code. The trellis structure of the code has a constraint length of 7, and the code generator polynomials of 171 and 133 (in octal numbers), with a rate of 1/2. The encoded bit stream is modulated by a real-valued binary phase-shift keying (BPSK) signal alphabet $\mathcal{C} = \{-1, +1\}$. The BPSK-modulated signal is upsampled by a factor $P = \lceil f_{\mathrm{s}}/\mathrm{BW} \rceil$ before going through

the TX filter. The TX filter is a low pass Hamming filter with bandwidth BW $= 5$ kHz and length 501 that shapes the modulated baseband signal. Moreover, there is an amplitude modulation, omitted in Fig. 1, that shifts the baseband signal to $f_c = 7.5$ kHz, generating the passband signal. Then, the message to be transmitted is concatenated with a pilot signal used for synchronization purposes. This pilot consists of a chirp signal with 184 ms, whose frequency varies linearly from 5 kHz to 10 kHz, plus a 92 ms guard time that is used to avoid interference between the chirp and the signal. Finally, the block is completed with a guard time period, used to ensure that there is no interference among blocks. A complete transmitted block is shown in Fig. 4.

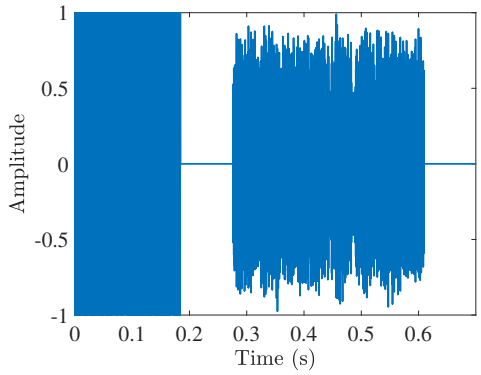

Fig. 4. One block of the transmitted signal.

C. Digital Receiver

The receiver task is to obtain the best estimate of the original message. The first step in the digital back-end receiver is filtering the received signal for mitigating interferences from signals outside the frequencies of interest. For this purpose, a digital bandpass filter (5-10 kHz) was applied to the signal. As the sampling frequency is f_s = 96 kHz. The signal is then downsampled by a factor $Q = 4$, for better use of computational resources. The result is a sampling frequency f'_s = 24 kHz. After filtering and downsampling, the received signal is split into blocks.

Synchronization is vital in this communication system. Each block is treated separately in the digital back-end receiver, so the signal stream has to be correctly split. This step is omitted in Fig. 1, but it is essential for a successful practical transmission. The synchronization step is depicted in Fig. 5: a cross-correlation is computed between the received signal and the chirp contained in the pilot signal. Since every block has its chirp, the correlation results in peaks marking the beginning of each block. Thus, the block detector divides the signal into blocks, each one containing chirp, guard time, and message. An example of the block detector output is illustrated in Fig. 6.

Within each block, the received message is separated from guard time and chirp to be processed. The RX filter at the receiver transforms the passband message into baseband. From baseband symbols, the vector is filtered again by pulse shaping filter then downsampled $P' = \lceil f'_s/\mathrm{BW} \rceil$ times. Next stage is equalization which was discussed in details in Section III. However, the equalizers need information about the channel to

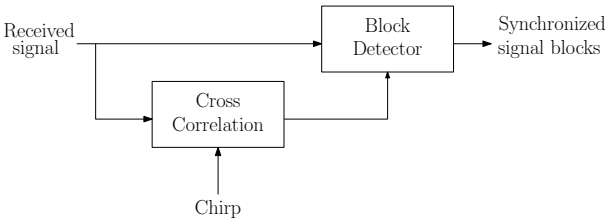

Fig. 5. Synchronization process.

be employed. Thus, the channel impulse response is estimated, modeling the problem as a linear convolution between the transmitted and received block. The channel impulse response is computed solving the linear convolution using a least squares approach. The equalized signal is demapped into bits and goes into the channel decoder using a soft Viberti algorithm [10], yielding the estimated transmitted message.

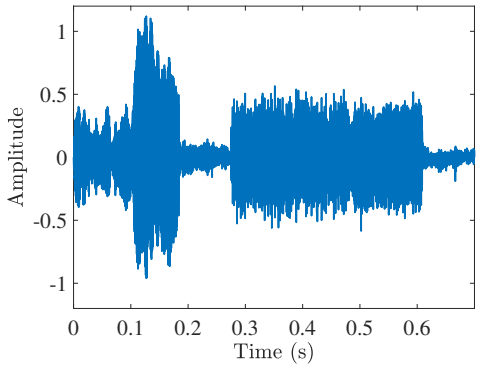

Fig. 6. One block of the received signal.

V. Results

The performance of the equalizers are evaluated in three different ways: a qualitative measure of the received image in each data block, the MSE between the originally transmitted image and the received image in each data block, and a bit-error rate analysis. All these results are reported as functions of the SNR. In this experiment, the SNR is defined as the signal power at the receiver over the noise power, where the noise power is calculated during guard time. The measured SNR obtained in this experiment was approximately 10 dB. However, to create diversity in the results, we introduced AWGN noise in the received signal, varying the SNR range from -4 dB to 10 dB, with a step of 2 dB.

The first results presented are the mean received images. The mean received image is computed as the mean of the images calculated from all the 115 received blocks. Fig. 7 shows the mean received images for SNR $= 10$ dB, which was the SNR observed during the experiment. For comparison purposes, the same results are presented for SNR $= 5$ dB in Fig. 8. Visually, the results for SNR $= 5$ dB are different, showing that the system using the DFE gives the best average image. However, these analyses are qualitative; to give a quantitative result the MSE is calculated. The MSE presented is the MSE between the transmitted image and the computed images for every block at the receiver. TABLE I presents the MSE for SNR $= 5$ dB and SNR $= 10$ dB, which shows

that the DFE is the equalizer that provides an image closer to the transmitted image when compared to the ZF and MMSE equalizers.

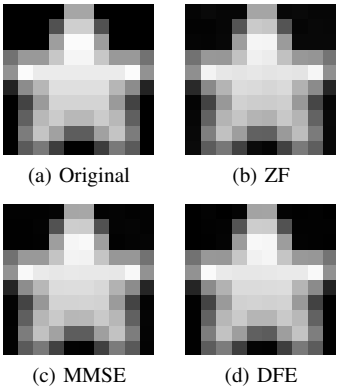

(a) Original (b) ZF

(c) MMSE (d) DFE

Fig. 7. Transmitted image and the computed in the receiver, SNR = 10 dB.

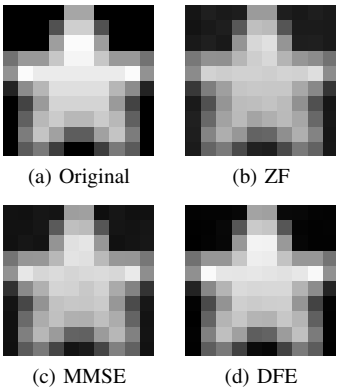

(a) Original (b) ZF

(c) MMSE (d) DFE

Fig. 8. Transmitted image and the computed in the receiver, SNR = 5 dB.

TABLE I

MSE OF THE IMAGES COMPUTED IN THE RECEIVER.

	MSE (dB)	
Equalizer	SNR = 5 dB	SNR = 10 dB
ZF	−12.6	−21.3
MMSE	−14.9	−23.7
DFE	−19.4	−25.6

Fig. 9 shows the average BER for all the data transmitted. The MMSE equalizer had a better performance than the ZF equalizer, having an SNR gain of 2.1 dB. The MMSE equalizer always performs better than the ZF equalizer in noisy environments, since the MMSE equalizer takes into account the additive noise and compensates it, avoiding noise enhancement. The DFE outperformed both ZF and MMSE equalizers, achieving lower BER and having an SNR gain of 5.3 dB over the ZF equalizer, and 3.4 dB over the MMSE equalizer. The more robust approach to the ISI problem by the DFE makes its performance the best.

VI. CONCLUSIONS

This work has shown a detailed view of data preparation for UWA transmission and reception, in which the use of equalizers was emphasized. All experiments were carried out in a real scenario in shallow water communication near the shore of the city of Arraial do Cabo. The ZF equalizer, the MMSE equalizer, and the DFE were employed to mitigate ISI

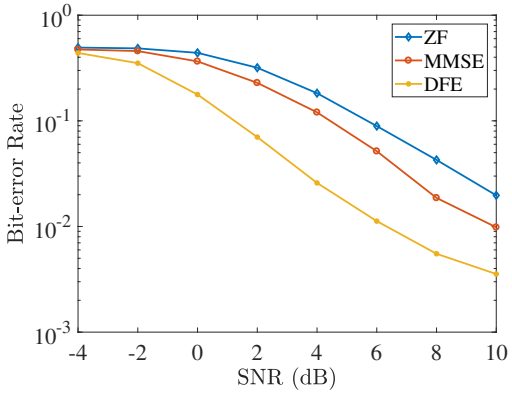

Fig. 9. BER performance of ZF equalizer, MMSE equalizer and DFE.

and improve BER. The DFE had the best performance among the equalizers, improving BER by 5.3 dB with respect to the ZF equalizer, and 3.4 dB with respect to the MMSE equalizer.

ACKNOWLEDGMENTS

We would like to thank the Institute of Sea Studies Admiral Paulo Moreira for the collaboration. We also would like to thank the talented Gabriel Chaves for helping us with Fig. 3.

REFERENCES

[1] C. M. G. Gussen, P. S. R. Diniz, M. L. R. Campos, W. A. Martins, F. M. Costa, and J. N. Gois, "A Survey of Underwater Wireless Communication Technologies," *Journal of Communication and Information Systems*, vol. 31, no. 1, pp. 242–255, 2016.

[2] X. Lurton, *An Introduction to Underwater Acoustics: Principles and Applications*, 2nd ed. Chichester: Springer, 2010.

[3] D. Brady and J. C. Preisig, "Underwater Acoustic Communications," vol. 4, pp. 330–379, November, 1998.

[4] B. Katsnelson, V. Petnikov, and J. Lynch, *Fundamentals of Shallow Water Fundamentals of Shallow Water Acoustics*. Boston: Springer, 2012.

[5] C. Liu, Y. V. Zakharov, and T. Chen, "Doubly Selective Underwater Acoustic Channel Model for a Moving Transmitter/Receiver," *IEEE Transactions on Vehicular Technology*, vol. 61, no. 3, pp. 938–950, February, 2012.

[6] P. A. van Walree, "Propagation and Scattering Effects in Underwater Acoustic Communication Channels," *IEEE Journal of Oceanic Engineering*, vol. 38, no. 4, pp. 614–631, October 2013.

[7] D. Kilfoyle and A. Baggeroer, "The State of the Art in Underwater Acoustic Telemetry," *IEEE Journal of Oceanic Engineering*, vol. 25, no. 1, pp. 4–27, January 2000.

[8] M. Stojanovic, "Recent Advances in High-speed Underwater Acoustic Communications," *Oceanic Engineering, IEEE Journal of*, vol. 21, no. 2, pp. 125–136, April, 1996.

[9] R. S. Chaves, W. A. Martins, and P. S. R. Diniz, "Modeling and Simulation of Underwater Acoustic Communication Systems," in *XXXV Simpósio Brasileiro de Telecomunicações e Processamento de Sinais*, São Pedro, September, 2017.

[10] J. G. Proakis and M. Salehi, *Digital Communications*, 5th ed. New York: McGraw-Hill Education, 2007.

[11] S. Haykin, *Communication Systems*, 4th ed. New York: John Wiley & Sons, Inc., 2001.

[12] C. A. Belfiore and J. H. Park, "Decision Feedback Equalization," *Proceedings of the IEEE*, vol. 67, no. 8, pp. 1143–1156, August, 1979.

[13] N. Al-Dhahir and J. Cioffi, "MMSE Decision-Feedback Equalizers: Finite-length Results," *IEEE Transactions on Information Theory*, vol. 41, no. 4, pp. 961–975, July 1995.

[14] P. S. R. Diniz, W. A. Martins, and M. V. S. Lima, *Block Transceivers: OFDM and Beyond*. Colorado Springs: Morgan & Claypool Publishers, 2012.

[15] M. E. Austin, "Decision-feedback Equalization for Digital Communication Over Dispersive Channels." *MIT Lincoln Laboratory*, August, 1967.

[16] P. Voois, I. Lee, and J. Cioffi, "The Effect of Decision Delay in Finite-length Decision Feedback Equalization," *IEEE Transactions on Information Theory*, vol. 42, no. 2, pp. 618–621, March 1996.